Cell Reports
Physical Science

Article

Identifying key drivers of product formation in microbial electrosynthesis with a mixed linear regression analysis

Graphical abstract

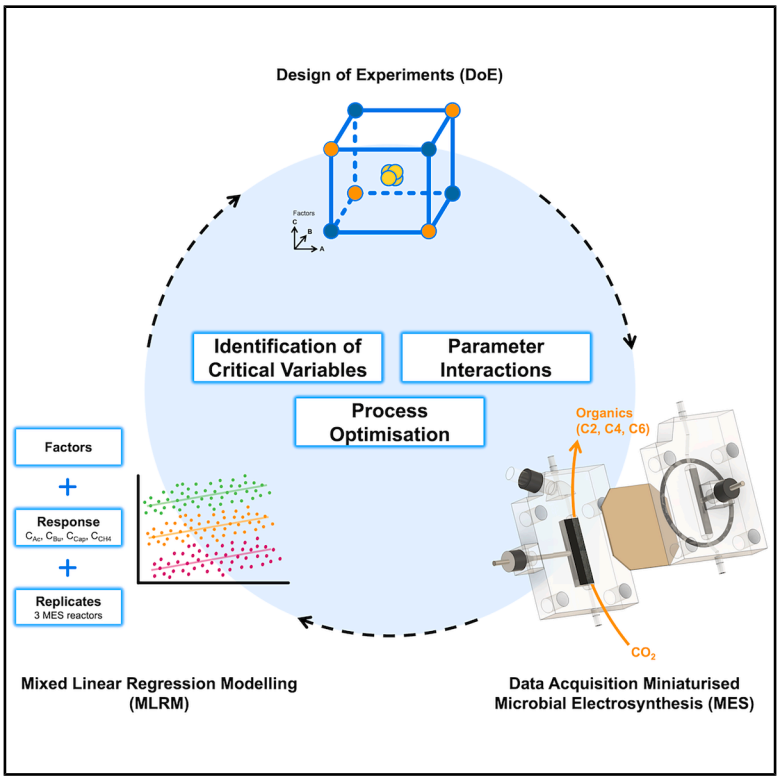

Authors

Marika Alida Johanna Zegers, Moumita Roy, Ludovic Jourdin

Correspondence

l.jourdin@tudelft.nl

In brief

Zegers et al. present a statistical roadmap for microbial electrosynthesis, combining design of experiments and mixed linear regression to identify pathway drivers. The analysis identifies CO_2 and pH as key for carbon fixation, highlights acetate availability for elongation, and reveals selenium and tungsten as enhancers of butyrate and caproate formation.

Highlights

- DoE and MLRM reveal key factor effects and interactions in biofilm-driven MES
- CO_2 availability drives acetate and indirectly enables downstream chain elongation
- Acetate availability and microbial activity jointly determine elongation selectivity
- Se/W enhance butyrate and caproate selectivity, indicating faster chain elongation

Zegers et al., 2025, Cell Reports Physical Science 6, 102934
November 19, 2025
https://doi.org/10.1016/j.xcrp.2025.102934

CellPress

Cell Reports
Physical Science

CellPress
OPEN ACCESS

Article

Identifying key drivers of product formation in microbial electrosynthesis with a mixed linear regression analysis

Marika Alida Johanna Zegers,[1,2] Moumita Roy,[1,2] and Ludovic Jourdin[1,2,3,*]
[1]Department of Biotechnology, Delft University of Technology, van der Maasweg 9, 2629 HZ Delft, the Netherlands
[2]e-Refinery Institute, Delft University of Technology, Leeghwaterstraat 39, 2628 CB Delft, the Netherlands
[3]Lead contact
*Correspondence: l.jourdin@tudelft.nl
https://doi.org/10.1016/j.xcrp.2025.102934

SUMMARY

Defossilization of industrial processes has led to a growing interest in alternative biotechnologies capable of producing chemicals from renewable resources. Microbial electrosynthesis (MES) is an emerging technology in which electrotrophic microorganisms utilize electrons from a cathode and CO_2 to produce multi-carbon compounds. To reach industrial application, clearer insights into the interactions between underlying biological, electrochemical, and physicochemical processes are required. Although individual parameters have been widely studied, identifying the most influential factors and their interactions remains challenging. This study applies design of experiments (DoE) and mixed linear regression modeling (MLRM) to examine the influence of pH, CO_2 and H_2 partial pressures, acetic acid concentration, and the addition of tungsten and selenium on the production spectrum in biofilm-driven MES. The developed DoE-MLRM approach highlights the key role of pH and CO_2 availability in supporting carbon fixation and acetate production, while the trace metals selenium and tungsten mostly promote chain elongation.

INTRODUCTION

The Paris Agreement aims to limit climate change by reducing greenhouse gas emissions, over 78% of which come from the use of fossil fuels, particularly in energy and chemical production.[1] While the transition to renewable energy sources such as wind and solar power has reduced CO_2 emissions from energy production, the chemical industry faces unique challenges due to its reliance on fossil fuels as both a source of energy and carbon.[2] To address this challenge, sustainable alternatives, such as renewable organic sources or CO_2, are being investigated.[3] Microbial electrosynthesis (MES), a technology that uses microorganisms as biocatalysts to reduce CO_2 to organic carbon compounds, is a promising method for sustainable chemical production. Unlike traditional electrochemical methods, which are limited to the production of C1 and C2 compounds, MES can facilitate the formation of larger carbon molecules, including carboxylates and alcohols.[4–7] This makes MES a potential tool for sustainable carbon capture and utilization, helping to achieve global climate goals.

To date, MES research has mainly focused on advancing the technology by studying fundamental aspects, such as electron transfer mechanisms and CO_2 reduction pathways, or improving the efficiency of key components, such as the microbial culture and cathode structure/material.[8,9] Although significant progress has been made, a deeper understanding of the interplay between different complex processes (biological, physical, electrochemical, and chemical) within MES systems is required to ultimately push the technology toward industrial implementation. One such example is the comprehensive understanding of the relationships between various operational conditions and microbial metabolism. The effect of single operational parameters, such as cathode potential, pH, inorganic carbon source, nutrient availability, H_2 partial pressure, and temperature, on MES efficiency has been extensively studied.[10–13] However, it has proven difficult to identify the most influential operating parameters in functioning MES systems in order to understand how different conditions interact with each other. Mathematical modeling could provide a systematic approach to assess the complexity of an MES system while complementing relevant experimental research.[14]

In recent years, several studies have been published on modeling MES, also on the dynamics between operating conditions and the microbial response. Gadkari et al.[15] presented a dynamic computational model for a two-chamber H-type MES system operated as a batch, focusing on the impact of operational parameters on MES performance. The model showed that, for MES operations with a cycle time of 3–4 days, increasing the initial substrate concentrations at the anode and cathode linearly increased the product formation rate. A trade-off between product formation rate, substrate consumption, and Coulombic efficiency highlighted the importance of multi-objective optimization. Another study demonstrated that machine learning algorithms, particularly XGBoost, can effectively predict acetate and

ethanol yields in MES based on operational factors such as cathode material, pH, applied potential, temperature, and inorganic carbon (IC) concentrations.[16] Experimental data were acquired with a batch-operated glass H-type dual-chamber reactor. Feature importance analysis identified current, pH, and IC as key parameters, while traditionally influential factors like applied potential and temperature had a lesser impact. Cabau-Peinado et al.[17] presented a computational model for MES that predicted microbial growth, current consumption, and CO_2 reduction to acetate, n-butyrate, and n-caproate by linking microbial metabolism to electrochemical processes. The model results suggested that CO_2 concentration might limit existing MES systems, highlighting the need for effective CO_2 delivery methods. Additionally, in biofilm-based reactors, continuous operation appeared to enhance microbial growth, support denser biofilm formation, and increase current densities.

Although all of these models are based on working MES systems and trained on the data obtained from them, no direct evidence has been provided from running MES reactors on how the microbial community adapts to changing operating parameters and to different reactor environments. In this context, design of experiments (DoE) can be used, a systematic method used to plan, conduct, and analyze experiments in order to understand the effects of multiple variables on an outcome. By varying different factors within an experiment together, DoE allows one to determine how these factors individually and interactively influence the results. DoE is commonly used to optimize processes, identify critical variables, and develop predictive models across fields like engineering, manufacturing, biotechnology, and social sciences. It is particularly valuable for identifying the most influential parameters, improving process efficiency, and achieving robust, reproducible results.[18]

Among the wide array of operational parameters, pH, CO_2 availability, and H_2 production emerge as critical factors due to their direct influence on microbial activity and system performance in MES reactors. Local pH changes near the cathode, driven by the hydrogen evolution reaction, create an alkaline environment that can significantly affect microbial activity and viability. These shifts also affect substrate availability, as they alter the HCO_3^-/CO_3^{2-} equilibrium and the solubility of CO_2. While buffers can mitigate these effects, their diffusion into the boundary layer becomes limiting at higher current densities.[19] CO_2 loading rate alone has been shown to strongly affect bioelectrochemical chain elongation.[20] High CO_2 loading rates (173 L d^{-1}) favor the production of butyrate and n-caproate over the production of acetate, whereas low CO_2 loading rates (8.6 L d^{-1}) result predominantly in acetate production, even with an extended retention time. When pH and CO_2 loading rate are pushed to their extremes, such as at low pH or under limited electron acceptor availability, microbes may activate alternative metabolic pathways.[21] For example, acetogenic bacteria may shift from acetogenesis to solventogenesis under these conditions.[22] H_2 availability is another critical parameter in MES, as acetogenic bacteria depend on dissolved H_2 concentration to drive acetogenesis, with rates increasing linearly under first-order kinetics.[23] Maintaining sufficient H_2 levels ensures efficient CO_2 conversion, directly impacting system performance. Finally, medium composition is another crucial yet underexplored factor in MES systems. Metalloenzymes involved in the Wood-Ljungdahl pathway (WLP) depend on cofactors like selenium (Se) and tungstate (W), which have been shown to improve the activity of this pathway.[24–26] Incorporating these cofactors in the catholyte medium could enhance microbial efficiency, complementing the optimization of operational parameters such as pH, CO_2, and H_2 availability.

In many experimental designs, two or more variables are related, and it is of interest to model and explore this relationship. The relationship between dependent (response) variables and independent (regressor) variables is characterized by a mathematical model called a regression model, which is fit to a set of sample data.[18] Regression methods are highly valuable in designed experiments, particularly when unexpected issues arise, such as missing observations, providing a robust framework for data analysis and interpretation. In many MES studies, data are obtained from multiple reactors, each representing a distinct experimental condition or grouping. In such cases, traditional regression models may fall short, as they assume independence of observations and do not take into account possible correlations within groups. Mixed linear regression models (MLRMs) offer a robust framework for addressing these challenges by incorporating both fixed effects, which capture overall trends across all groups, and random effects, which account for variability within and between groups.[27] This approach allows for the simultaneous analysis of overall trends and group-specific deviations, making it particularly suitable for data arising from multiple experimental reactors.

This work highlights the implementation of DoE and MLRMs to determine the influence of pH, CO_2 partial pressure (pCO_2), H_2 partial pressure (pH_2) and the addition of W and Se on the production spectrum of biofilm-driven, miniaturized, directed flowthrough bioelectrochemical systems (DFBRs).[28] By using a DoE-MLRMs approach, the importance of the interactions among the key parameters discussed above (pH, CO_2 loading rate, H_2 availability, and the addition of metalloenzymes) as well as their individual statistical significance can be systematically assessed, offering insights into their combined and independent effects on MES performance in operational reactors.

RESULTS AND DISCUSSION

From complex patterns to interpretable results with mixed linear regression

Two different experimental designs were developed to create three different models that assess the separate effect of a combination of factors on the production of the carboxylates acetate (C2), butyrate (C4), and caproate (C6) in biofilm-driven MES: (1) pH, pCO_2 and pH_2; (2) pH, pCO_2, and acetic acid concentration (c_{Hac}); and (3) the addition of Se and W in the trace metal solution. Three miniaturized DFBRs were subjected to the conditions described in the three experimental designs over the course of 63–95 days (Figure 1). Each experimental condition lasted for at least 2 hydraulic retention times (HRTs; 8 days) to observe possible trends in production of carboxylates over time. As illustrated in Figure 1, it would be difficult to identify clear trends without relying on speculation, due to the complexity and variability of the data. This highlights the need for a statistical

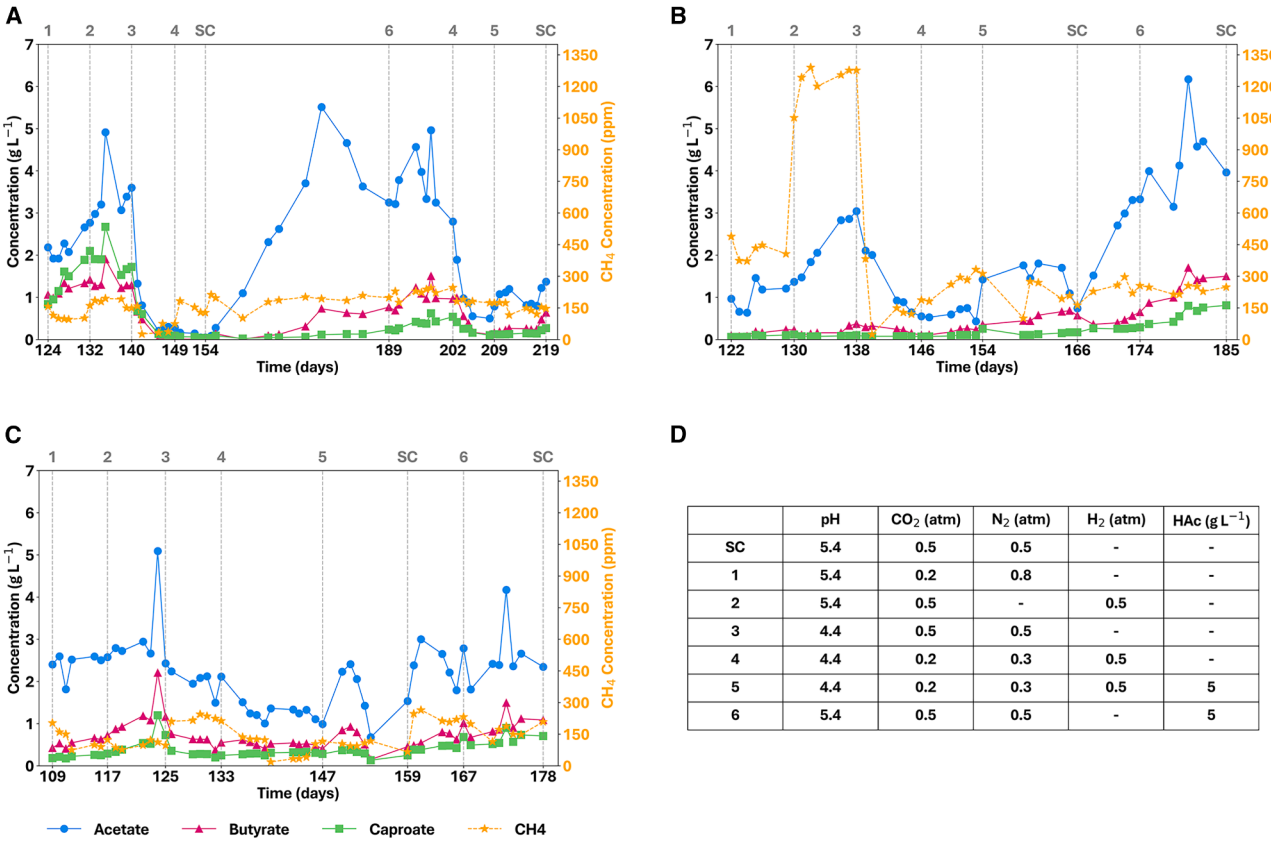

	pH	CO_2 (atm)	N_2 (atm)	H_2 (atm)	HAc (g L^{-1})
SC	5.4	0.5	0.5	-	-
1	5.4	0.2	0.8	-	-
2	5.4	0.5	-	0.5	-
3	4.4	0.5	0.5	-	-
4	4.4	0.2	0.3	0.5	-
5	4.4	0.2	0.3	0.5	5
6	5.4	0.5	0.5	-	5

Figure 1. Carboxylate and methane concentrations during DoE conditions in three continuous reactors

Shown are concentrations (g L^{-1}) of acetate (blue circles), butyrate (red triangles), caproate (green squares), and CH_4 (ppm; orange stars) during the different design of experiment (DoE) conditions for reactor 1 (A), reactor 2 (B), and reactor 3 (C). Each reactor was operated in continuous mode with a hydraulic retention time of 4 days. Vertical dotted lines indicate transitions between experimental conditions, each representing a specific combination of conditions (D). SC refers to the standard operating conditions under which the reactors are typically run. In reactor 1 (A), a pH control issue occurred on day 154, leading to a significant drop in pH and a recovery period before the experimental design could be completed.

approach such as MLRM, which allows for a more reliable interpretation of results across replicate experiments. For all three designed experiments, an MLRM approach was applied to determine which factors had a significant effect on production for each product separately.

pH and CO_2 supply affect carbon fixation and chain elongation

The main output of the MLRM, modeling pH, pCO_2, and additional bulk H_2, is presented in Table 1, while the concentration profiles of all carboxylates and CH_4 are shown in Figure 1 (conditions 1–4). The complete model output for each product is provided in Note S1, which also includes model validation checks (observed vs. predicted plots, residuals, and Q-Q plots). A description of the regression model validation methods and their interpretation is provided in Methods S4. For all tested independent variables (C2, C4, C6, and CH_4), the intercept is positive and significant, indicating that factors beyond those tested contribute to the production of those compounds. The estimated reactor-to-reactor variance ranges from 0.034 to 0.121 (SE = 0.175–0.376) for all carboxylic acids, which is approximately 31%–72% of the residual variance. In all cases, the SE of the reactor-specific variance estimate was larger than the estimate itself. This means there is considerable uncertainty about how much variation can be attributed to differences between reactors. This typically suggests that the variation between reactors is relatively small compared to the variation explained by the experimental conditions. In other words, the reactor had little influence on the outcome, and the observed effects are more likely driven by the tested variables (pH, pCO_2, and pH_2) rather than random differences between individual reactors. The conditional R^2 (R^2_c) is higher than the marginal R^2 (R^2_m) for all organics, indicating that reactor-to-reactor variability contributed to the total explained variance. This suggests that, beyond the effects of pH, pCO_2, and pH_2, reactor-specific factors, in particular variation in microbial community composition and biofilm development, may influence production.

The MLRM results in Table 1 indicate that acetate production in MES is primarily driven by pH and CO_2 availability, with both variables having statistically significant positive effects ($p < 0.001$). This aligns with known MES processes where a mildly acidic pH (5–6) promotes microbial conversion of CO_2 to carboxylic acids.[20,29–31] Additionally, since acetate is a weak acid, an increase in pH also reduces the fraction of

Table 1. Mixed linear regression results for pH, pCO_2, and pH_2

Compound	Intercept (P>|z|)	pH (P>|z|)	pCO_2 (atm) (P>|z|)	pH_2 (atm) (P>|z|)	Reactor var.	R^2_m	R^2_c
Acetate (C2)	<0.001	<0.001	<0.001	0.179	0.121	0.747	0.853
Butyrate (C4)	<0.001	0.005	0.282	0.517	0.034	0.379	0.527
Caproate (C6)	0.022	0.015	0.489	0.685	0.080	0.270	0.510
Methane (CH_4)	0.016	0.152	0.306	0.220	22755.222	0.212	0.447

Shown is main output from the MLRM assessing the effect of pH, pCO_2, and pH_2 on the production of acetate, butyrate, caproate, and CH_4. For the intercept, pH, pCO_2, and pH_2, the P>|z| is given, which refers to the p value for a z test of the null hypothesis that a given coefficient is zero. The reactor variance indicates how similarly reactors behave compared to each other under the tested conditions. R^2_m and R^2_m represent the marginal and conditional R^2, respectively.

undissociated acetic acid, preventing toxicity and allowing sustained production.[32] Looking at the regression coefficients for acetate (Note S1.1), pCO_2 has a larger effect size than pH, suggesting that increasing CO_2 availability is a key factor in maximizing acetate production. This observation aligns with the outcomes of the black-box kinetic model developed by Cabau-Peinado et al.,[17] which also identified dissolved CO_2 concentration as a limiting factor in MES systems. Acetate synthesis in MES is CO_2 dependent, primarily occurring via the WLP, where CO_2 is reduced to acetate.[33,34] At industrial scale, CO_2 availability can be enhanced through practical measures, such as increasing gas flow and partial pressure, using gas diffusion cathodes and/or membranes, and applying flowthrough reactor designs that ensure steady CO_2 delivery to biofilms.[29,35]

In contrast, additional bulk H_2 did not significantly impact acetate formation (p = 0.179), suggesting that additional bulk H_2 supply does not majorly influence system performance. Since the additional H_2 was supplied through the bubble column, mass transfer to the microorganisms could have limited additional dissolved H_2 to become available to the biofilm, preventing a strong response. While the regression coefficient is positive (Note S1.1), the lack of significance suggests that additional H_2 is not a major driver of acetate production under the tested conditions. These results indicate that hydrogen supplied from the cathode was sufficient to sustain acetate production within the biofilm without the need for external H_2 supplementation. Additionally, the addition of external H_2 did not lead to biofilm detachment or increased planktonic growth, as confirmed by stable optical density 600 (OD_{600}) measurements over time (Note S2).

For both butyrate and caproate, only the pH is associated with an increase in concentration ($p < 0.05$), suggesting that pH regulation is an important factor in optimizing their production. In MES-related technologies, such as syngas fermentation, a lower pH has been shown to inhibit chain elongation and can cause shifts toward ethanol or lactate production.[34] While the positive coefficient for CO_2 (Notes S1.2 and S1.3) suggests a possible beneficial effect of pCO_2 on butyrate and caproate, the lack of statistical significance ($p > 0.05$) indicates that this effect is not robust under the tested conditions. Although butyrate has been hypothesized to form directly from CO_2 in MES and syngas fermentation, both butyrate and caproate can also be produced from acetate via reverse β-oxidation.[30,36–38] For anaerobic bioprocesses, acetate reduction to butyrate and caproate have been determined to be thermodynamically and kinetically feasible when ethanol or lactate serve as electron donors.[39] Ethanol and lactate production was not observed in any reactors under any conditions in the liquid or gas phase, consistent with the findings of Jourdin et al.,[20] Cabau-Peinado et al.,[29] and Winkelhorst et al.[40] In the work by Jourdin et al.,[20] ethanol was not measured in significant concentrations, suggesting that direct electron transfer from the cathode or alternative metabolic pathways are involved in chain elongation. In that work, there were indications that ethanol was not a major electron donor, while CO_2 availability appeared to influence microbial metabolism, potentially favoring direct acetate utilization over ethanol-based elongation. The absence of detectable ethanol does not necessarily indicate its lack of involvement in chain elongation. In a gas fermentative system, ethanol has been shown to be consumed as quickly as it is produced or dosed, particularly in active chain-elongating microbial communities.[41,42] According to the current model, caproate synthesis seems to depend more on acetate and butyrate availability than direct CO_2 fixation due to its higher p value for pCO_2, unlike acetate and butyrate. CO_2 may still play a role as an upstream carbon source, but its impact on final caproate levels is likely indirect. The wide confidence interval (Notes S1.2 and S1.3) for the CO_2 rate in both products suggests, however, that additional interacting factors (e.g., electron availability or microbial community composition) may influence its impact, meaning that the current experimental design may not fully isolate the effect of CO_2 rate. Although H_2 is a key electron mediator in acetogenic and chain-elongating bacteria, additional supply of H_2 did not have a significant impact on chain elongation ($p > 0.05$).

Despite the addition of 2-bromoethanesulfonic acid (BES), CH_4 was still detected, which may be explained by consumption of BES by, for example, sulfate-reducing bacteria or by the gradual adaptation of methanogens to repeated dosing.[43–46] None of the three factors (pH, pCO_2, and additional bulk H_2) had a statistically significant effect on CH_4 production, as all p values considerably exceeded 0.05. The positive coefficients for all three factors suggest that higher values may promote CH_4 production, however, the wide confidence intervals indicate high variability and weak predictive power. This could mean that the methanogens present in the biofilm tolerate a wider pH range than other mesophilic methanogens (pH 6.5–8), making pH control alone insufficient to suppress methane production.[47–49] Moreover, the development of pH gradients within biofilms can create local variations in pH, which could also contribute to the persistence of methanogenic activity. Higher CO_2 availability alone does also not necessarily lead to more methane production, even though

Table 2. Mixed linear regression results for pH, pCO_2, and supplied acetic acid

Compound	Intercept (P>|z|)	pH (P>|z|)	pCO_2 (atm) (P>|z|)	Supplied HAc (g/L) (P>|z|)	Reactor var.	R^2_m	R^2_c
Acetate (C2)	<0.001	0.943	<0.001	0.042	<0.001	0.813	0.813
Butyrate (C4)	<0.001	0.021	<0.001	<0.001	<0.001	0.864	0.864
Caproate (C6)	<0.001	<0.001	<0.001	<0.001	0.006	0.764	0.899
Methane (CH_4)	<0.001	0.651	0.004	0.320	1480.729	0.299	0.715

Shown is main output from the MLRM assessing the effect of pH, pCO_2, and supplied acetic acid on the production of acetate, butyrate, caproate, and CH_4. For the intercept, pH, pCO_2, and Ac the P>|z| is given, which refers to the p value for a z test of the null hypothesis that a given coefficient is zero. The reactor variance indicates how similarly reactors behave compared to each other under the tested conditions. R^2_m and R^2_m represent the marginal and conditional R^2, respectively.

methanogens can use CO_2 and H_2 via hydrogenotrophic methanogenesis.[50] This means that the effect of CO_2 could have been masked by other untested factors. The high reactor variance indicates that reactor-specific factors (e.g., biofilm development, methanogen colonization, or slight differences in gas diffusion) may strongly impact CH_4 production. Suppression of methanogenesis might thus be more reactor dependent than process dependent, requiring targeted interventions at the microbial community level.

Acetic acid addition to the catholyte highlights its role in chain elongation

The previous model indicates that CO_2 primarily influences acetate concentration, highlighting its role in carbon fixation. Acetate is clearly a key intermediate in chain elongation, as there is a successive production pattern where acetate accumulates first, followed by butyrate and then caproate. To further investigate this relationship, another model was built to investigate the combined effects of CO_2, pH and supplementation of acetic acid (HAc) (5 g L^{-1}) to the reactor system on chain elongation. This approach aims to clarify whether CO_2 directly influences the production of butyrate and caproate or whether its primary function is limited to acetate synthesis, which then serves as the substrate for elongation.

The complete model output for each product is provided in Note S3, and a model summary is shown in Table 2. Note S3 also contains model validation checks (observed vs. predicted plots, residuals, and Q-Q plots). The concentration profiles of all carboxylic acids and CH_4 are shown in Figure 1 (conditions 4, 5, standard conditions [SC], and 6). For all independent variables (C2, C4, C6, and CH_4), the intercept is positive and significant, which means that factors other than the tested ones contribute to production of organics. The estimated reactor-to-reactor variance is 0–0.006 (SE = 0–0.102) for acetate, butyrate, and caproate (0%–130%) of the residual variance). Although the estimated reactor variance (0.006) exceeded the residual variance (0.0046) for the caproate model only, its large SE (0.102) indicates that reactor-to-reactor variability is either small or difficult to estimate reliably. Although some differences between reactors can be seen in the profiles, the model captures most of this variation as residual noise. With three reactors, it is difficult to reliably separate true reactor-specific effects from random variation, which is why the estimated variance appears smaller than what is visible in Figure 1. For all organics, the R^2_c was higher than the R^2_m, once more implicating that, beyond the fixed effects, reactor-specific factors influence microbial production.

From the results of the MLRM (Table 2), it is clear that the presence of added acetic acid reduced the apparent effect of pH (p = 0.943) on acetate concentration, since some acetate was externally supplied rather than microbially produced. CO_2 rate has a larger effect size than pH ($p < 0.001$), suggesting that CO_2 availability is the dominant driver of acetate synthesis, overshadowing any effects of pH. pH does not provide a carbon source like CO_2 but only influences enzyme activity and microbial growth, which might not be limiting in this scenario. This model once more highlights CO_2 as a key limiting factor for acetate production in MES, reinforcing the need for sufficient CO_2 supply to maximize acetate yield.

In this new MLRM, butyrate and caproate formation are shown once more to be pH sensitive, with p values for pH below 0.05. However, when compared to the MLRM with pH, pCO_2, and additional bulk H_2 as fixed effects (Table 1), a contradiction arises, as pCO_2 was not statistically significant for either chain elongation product in that model, whereas it is in this one. This contradiction can be explained by considering the metabolic pathways and interdependencies of acetate and butyrate production in MES. The MLRM results reveal a hierarchical structure in MES pathways. CO_2 availability is a key driver of acetate production ($p < 0.001$), while butyrate and caproate production depend on acetate availability, as indicated by the significance of added acetic acid ($p < 0.001$). pH influences acetate, butyrate, and caproate synthesis, reinforcing its role in maintaining optimal microbial activity. The contrasting significance of CO_2 between models suggests that the effect of CO_2 on chain elongation may be indirect. In previous literature, when acetate production has stabilized, limiting or intermittently feeding CO_2 can increase hydrogen partial pressure, thereby shifting the metabolic balance toward the reductive conversion of acetate into longer-chain products such as butyrate and caproate.[51,52] CO_2 availability may also influence microbial community composition, enriching for chain-elongating bacteria under more reducing conditions.[25,51,53] These findings highlight the importance of controlling CO_2 and acetate availability at different stages of MES to optimize chain elongation pathways.

In the first presented model (pH, pCO_2, and pH_2), methanogenic species were affected by none of the factors. In the current model, H_2 was not included, and acetic acid was added instead, which resulted in a significant effect for pCO_2 on methane production (p = 0.004). In a biofilm-driven MES system, more than 99% of microbes are present in the biofilm (Note S2), but some persist in the bulk liquid, meaning

competition for H_2 occurs at different spatial levels.[29] The difference in CH_4 production between the two models can be attributed to shifts in electron donor availability and microbial competition dynamics. In the first model, additional bulk H_2 (in the gas phase) and electrode-derived H_2 were available, leading to competition between methanogens and acetogens in both the biofilm and bulk liquid. This competition likely resulted in acetogens preferentially utilizing H_2, limiting CH_4 production and making CO_2 non-significant. This is an interesting observation, as methanogens generally have a lower hydrogen affinity (K_s) compared to acetogens, meaning they can utilize hydrogen at lower concentrations.[54] However, acetogens achieve higher conversion rates at elevated hydrogen partial pressures. Consequently, at higher hydrogen concentrations, acetogens can outcompete hydrogenotrophic methanogens. This is because the increased availability of hydrogen favors acetogenic pathways, leading to acetate production.[50] In the current model, the removal of additional bulk H_2 forced methanogens to become more dependent on CO_2, increasing its statistical significance as a driver of methane formation. Acetic acid addition did not significantly impact CH_4, suggesting that hydrogenotrophic rather than acetoclastic methanogenesis was dominant. 16S rRNA gene sequencing of the mixed culture inoculum revealed *Methanobrevibacter* as the most abundant methanogenic genus (Figure S29), which is generally considered hydrogenotrophic.[55,56] These results highlight the importance of both substrate availability and spatial distribution (biofilm vs. bulk) in regulating CH_4 formation in MES systems.

Addition of W and Se to the trace metal solution significantly improves carbon fixation and chain elongation

The availability of trace elements like Se and W is vital in MES, as these elements serve as cofactors for key enzymes in the WLP, and their presence can significantly impact the pathway's efficiency and the overall microbial productivity.[24–26,57] Formate dehydrogenase (FDH), which catalyzes the reduction of CO_2 to formate, often contains selenocysteine at its active site, which is crucial for its catalytic efficiency. Selenocysteine-containing FDHs exhibit higher catalytic rates compared to their non-selenium counterparts.[58] In certain acetogens, W can act as a cofactor for FDH.[58] In acetate-producing acetogens, the presence of Se and W in FDH has been suggested to function as a cofactor.[26,59] In gas fermentation processes, W has not only been shown to activate FDH but also aldehyde oxidoreductases and related enzymes, driving the production of more reduced intermediates like acetaldehyde and ethanol.[25,53] Ensuring an adequate supply of these trace metals in the growth medium can enhance the catalytic capability of FDH, leading to improved conversion rates of CO_2 to desired products. A simplified MLRM was used to gain key insights into whether the addition of W and Se has a significant effect on carbon fixation to acetate and whether it had any impact on the following chain elongation reactions. The production spectrum of each reactor before (1) and after (3) the addition of Se and W is presented in Figure 2. The full output and validation checks of the simplified model are provided in Note S4 for each product, and a model summary is presented in Table 3.

For all independent variables (C2, C4, and C6) the intercept is positive and significant, meaning that their change in concentration is not solely due to the absence and addition of Se and W. The reactor variance for acetate was 0.008, but its large SE (0.707) suggests that this estimate is unreliable, implying that most acetate variation is due to residual noise rather than systematic reactor differences. In contrast, butyrate and caproate production had zero reactor variance (SE = 0). This does not imply that the reactors were identical but, rather, that with only three groups, the model could not reliably distinguish reactor-specific variability from residual error. The lower residual variances for butyrate (0.1008) and caproate (0.1712) compared to acetate (0.6564) suggest that chain elongation products were less affected by random variation.

From the simplified MLRM, the acetate concentration in the system was positively, but not significantly, affected by the addition of the trace metals Se and W to the system (p = 0.139). This seems to be a contradictory observation, as Se and W are key co-factors for FDH in the WLP. One possibility is that acetate production was not strongly limited by trace metal availability, suggesting that the current medium composition provided enough trace metals for the WLP to run sufficiently. On the other hand, this seems unlikely, as Se and W have been shown, in processes other than MES, to improve acetate production through the WLP.[24–26,60] The MLRM results for butyrate and caproate provide insight into why the effect of trace metals appears to be insignificant for acetate. It is likely that acetate is being actively consumed by chain-elongating microbes to produce longer-chain products. The effect of Se and W on butyrate and caproate is not only positive, but the effect is also significant ($p < 0.05$). The R^2_m (0.325) and R^2_c (0.422) for caproate are the highest among all products, suggesting that trace metals play a more crucial role in caproate synthesis than in acetate and butyrate formation. If the addition of Se and W improves acetate production, then acetate consumption for butyrate and caproate formation also rises, thereby masking a net increase in acetate concentration. As a result, a clear statistical effect (significance) in butyrate and caproate concentrations is obtained, while acetate's net concentration might not show a significant increase because it is both produced and consumed at higher rates. This suggests that trace metals enhance multiple steps in MES, driving both acetogenesis and subsequent chain elongation, with the net effect being most visible in the final products rather than in the intermediate (acetate).

Figures 2B and 2C also illustrate the enhanced selectivity toward butyrate and caproate following the addition of Se and W to the catholyte medium, with concentrations reaching 2.21 and 3.79 g L^{-1} for butyrate and caproate in R2 and 2.54 and 2.52 g L^{-1} in R3, respectively. As mentioned before, Se and W enhance the conversion of CO_2 to acetate and reducing equivalents by activating specific enzymatic pathways at both the start of the metabolic pathway (CO_2 fixation) and further reduction steps. The effect of this could be an increased amount of usable acetate and reducing equivalents, like ethanol, in the system. Secondary fermenters in the mixed microbial community can

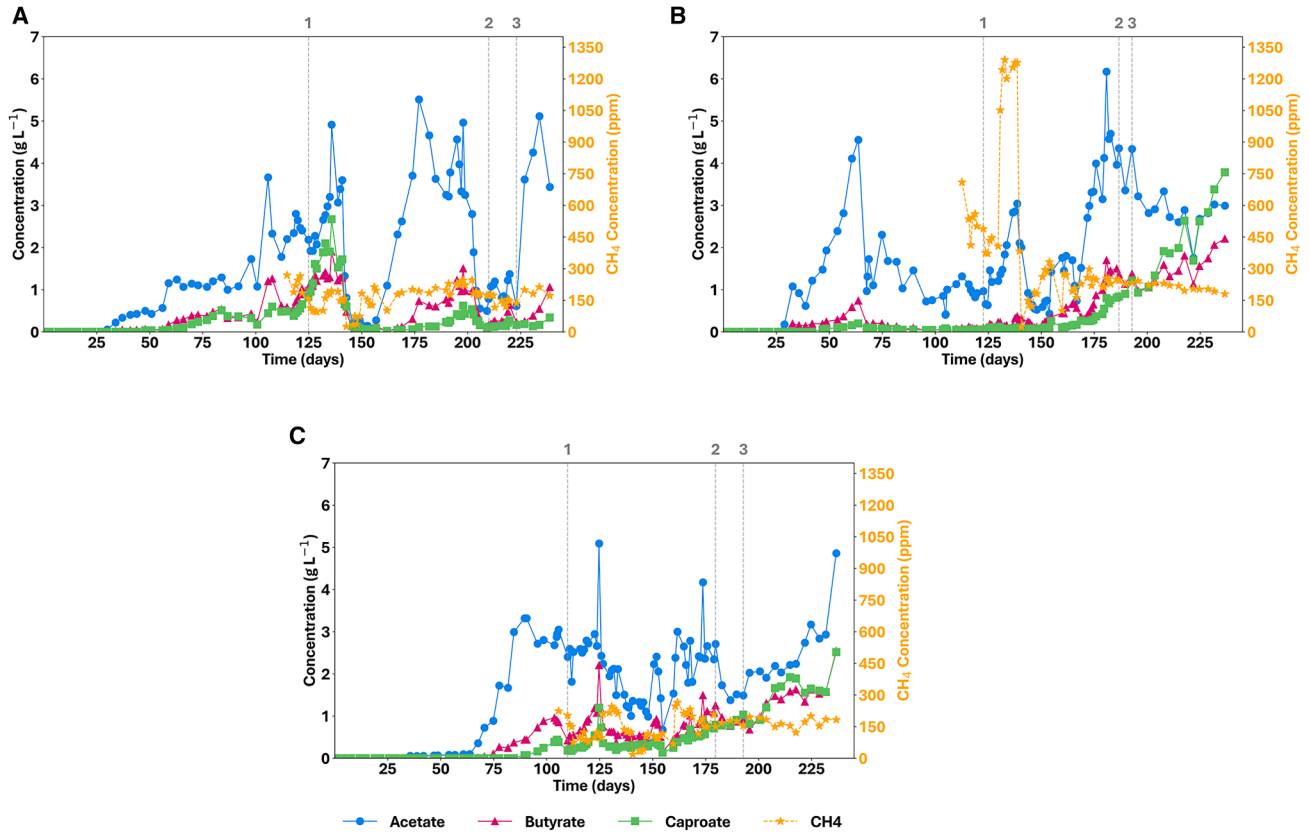

Figure 2. Carboxylate and methane concentrations before and after Se and W addition in three continuous reactors

Shown are concentrations (g L^{-1}) of acetate (blue circles), butyrate (red triangles), caproate (green squares), and CH_4 (ppm; orange stars) during 236–238 days for reactor 1 (A), reactor 2 (B), and reactor 3 (C). Vertical dotted lines indicate (1) the start of design of experiments (DoE), (2) end of DoE, and (3) addition of Se and W to the trace metal solution.

use these available compounds to perform chain elongation; for example by coupling ethanol oxidation to acetate reduction to generate butyrate and caproate. In gas fermentation, the presence of Se and W has been linked to higher ethanol:acetate ratios, higher total acid production, and onset of solventogenesis and chain elongation phases that are absent in their deficiency.[53,61] However, as mentioned previously, ethanol was not detected in any of the reactors, though its presence cannot be ruled out. In the current MES reactors, the presence of Se and W may intensify this dynamic by enhancing ethanol production and accelerating chain elongation, thereby reinforcing the likelihood of direct ethanol consumption without measurable buildup.

The opportunities for the use of DoE and MLRM in MES are endless

In this work, three different MLRM models were presented, all with different investigated factors and a different range of complexity. Due to the complexity of electrochemical systems and microbial interaction in mixed microbial cultures, the opportunities for the use of DoE and MLRM are virtually limitless. These experimental and statistical approaches can systematically deconstruct the influence of multiple interacting factors. This work only discusses the use of DoE and MLRM modeling to gain insight in how to shift and optimize the production spectrum, but the same approach can be applied to other aspects of MES, such as reactor design, microbial community engineering, process stability, and scale-up strategies.

MES systems often rely on biofilm formation at electrodes to enable efficient electron transfer. However, the microbial community composition plays a critical role in determining whether electrons flow toward acetate, butyrate, caproate, or methane. DoE and MLRM could be used to understand how biofilm thickness, electrode colonization, and microbial diversity impact product formation. As MES operates at the interface of microbiology and electrochemistry, DoE and MLRM could also be used to model how variations in electrode potential influence electron transfer efficiency and product selectivity, how current density affects microbial metabolism and growth, and how different electrode materials influence biofilm attachment and electrocatalysis. Another example of how DoE and MLRM can be used in MES is to assess the impact of scale-up factors, such as mass transfer and current distribution, on microbial performance. In practice, the scale-up factor can be included as an additional design variable (e.g., surface-to-volume ratio or electrode area relative to volume), allowing its effect and interactions with operational parameters to be quantified. These few

Table 3. Mixed linear regression results for Se and W addition

Compound	Intercept (P>|z|)	Se/W (P>|z|)	Reactor var.	R^2_m	R^2_c
Acetate (C2)	<0.001	0.139	0.008	0.265	0.274
Butyrate (C4)	<0.001	0.050	<0.001	0.391	0.391
Caproate (C6)	<0.001	0.037	0.001	0.419	0.422

Shown is main output from the MLRM assessing the effect of adding Se and W to the catholyte medium on the production of acetate, butyrate, caproate, and CH_4. For the intercept and Se/W, the P>|z| is given, which refers to the *p* value for a z test of the null hypothesis that a given coefficient is zero. The reactor variance indicates how similarly reactors behave compared to each other under the tested conditions. R^2_m and R^2_m represent the marginal and conditional R^2, respectively.

examples already highlight the wide extent to which this approach can be used.

There are methods for exploring non-linear relationships and optimizing process conditions, such as response surface methodology (RSM). RSM needs different and more complex DoE structures, such as central composite design and Box-Behnken, to fit quadratic models. These models also require more data compared to regression models and are less robust to missing/unbalanced data, as they rely on a structured experimental design with complete datasets.

Chaitanya et al.[60] investigated the optimization of volatile fatty acid (VFA) production from CO_2 in MES using RSM. It examined the effects of key operational parameters, including pH, gas pressure, ethanol concentration, electrolyte concentration, and trace elements, on VFA synthesis using mixed anaerobic consortia. However, the study utilized 100 mL serum batch bottles, which are inherently non-scalable for industrial applications due to several limitations. The focus of this study was to identify significant factors influencing the production of products in MES and find possible interactions between factors in a miniaturized version of a scalable reactor design (DFBR), making a mixed linear regression approach more suitable. Additionally, as MES studies generally run over extended periods of time, a straightforward yet insightful method could significantly reduce experimental time by identifying key variables and conditions early on, allowing researchers to refine parameters efficiently without the need for extensive approaches or elaborate experimental designs.

DoE and statistical models are valuable for research, as they are integral to the biotechnological industry, enhancing the efficiency and effectiveness of research and development processes. These methodologies facilitate the systematic planning and analysis of experiments, enabling researchers to extract maximum information with minimal resource expenditure. As MES progresses toward industrial implementation, DoE and MLRM will be instrumental in scaling up systems, ensuring reproducibility, and engineering microbial communities to drive CO_2 conversion toward valuable biochemicals with high efficiency and selectivity.

METHODS

MES reactor setup

Three miniaturized DFBRs (R1, R2, and R3) were assembled.[28] Each reactor contained a cathode and anode compartment, separated by a cation exchange membrane (CMI-7000s, Membrane International) and an NBR O ring. All components were 3D printed using a biocompatible resin (BioMed Clear Resin V1, Formlabs) with the Form 3B printer. The carbon felt cathode had a total volume of 1 cm^3 (4 × 0.5 × 0.5 cm) and a projected surface area of 2 cm^2. The anode was a titanium plate coated with Pt/IrO_2, supplied by Magneto Special Anodes (Schiedam, the Netherlands).

A bubble column, which was also 3D printed, was installed in the catholyte recirculation loop, allowing a mixture of CO_2 and N_2 to be sparged into the catholyte. To maintain the catholyte at a pH of 5.4, a pH controller (AQUIS Touch S, Jumo) was connected to a pH probe (QP108X, ProSense, the Netherlands) positioned in the recirculation circuit. The total catholyte volume, including the cathode chamber, bubble column, and all recirculation loop tubing, was 15 mL. To prevent phototrophic growth and keep the temperature at 30°C, the reactors were placed inside a heated cabinet, shielded from light.

MES reactor operation

The catholyte and anolyte medium composition can be found in the supplemental methods. The reactors were operated in continuous mode with an HRT of 4 days, and the recirculation rate for both the anolyte and catholyte was maintained at 2.10 L h^{-1}. Under standard conditions, a 50:50 CO_2/N_2 mixture was sparged through the cathodic bubble column at 0.05 L min^{-1} to provide dissolved CO_2 to the catholyte. All reactors were connected to a multi-channel potentiostat (BioLogic, France) in a three-electrode configuration, allowing for abiotic electrochemical testing and controlled operation post inoculation. A 3M Ag/AgCl reference electrode (QM710X, ProSense, the Netherlands) was used in each reactor.

Inoculation and biotic operations

Before inoculation, the MES reactors were abiotically tested with the methods outlined by Zegers et al.[28] Reactors 2 and 3 in this study correspond to reactors 2 and 3 described in this previous work. After characterization, the cathode potential was set to −0.9 V vs. SHE. Each reactor was inoculated with approximately 9.36 mg L^{-1} of biomass, comprised of a mixed microbial culture sourced from previously operated MES reactors that had produced acetate, n-butyrate, and n-caproate from CO_2.[29,40] When the pH was dropped from 5.4 to 4.4, the potential was corrected accordingly to −0.84 V vs. SHE.

Analytical methods

Biofilm growth and product formation were monitored by collecting 1.5 mL liquid samples from each reactor twice a week or daily (excluding weekends) depending on the

experimental conditions. The OD of unfiltered samples was measured at 600 nm with a UV-visible spectrophotometer (UV-1800 series, Shimadzu, Japan) to estimate planktonic cell concentrations. Biomass-specific growth rates and biomass-specific productivity were determined as described by Winkelhorst et al.,[40] where the total nitrogen (TN) content of centrifuged samples (20 min, 13,300 rpm) was measured using a TOC analyzer coupled to a TN unit (TOC-L series, Shimadzu) and was kept at an oven temperature of 720°C.

The concentrations of C2-C6 carboxylic acids and alcohols were analyzed using a gas chromatograph (Thermo Fisher Scientific, USA) with a Stabil-wax column (25 m length, 0.2 μm internal diameter). The column temperature was initially held at 50°C for 7 min, increased to 180°C for 8 min, and maintained at 180°C for 9 min. Helium (He) was used as a carrier gas, and the flame ionization detector (FID) was kept at 250°C. Methane presence was tested by collecting duplicate gas samples from the cathode recirculation circuit's bubble column either daily (excluding weekends) or twice weekly using glass vials. The samples were injected into a Trace1300 gas chromatograph (Thermo Fisher Scientific) equipped with a TriPlus RSH autosampler. The column temperature was initially held at 50°C for 5 min and increased to 175°C for 15 min. Hydrogen (H_2) was used as a carrier gas, and the FID was kept at 250°C.

Statistical analysis

Two different experimental designs were built. For the first model, pH, pCO_2, and supplied pH_2 were chosen as independent variables, while for the second model, pH, pCO_2, and supplied c_{HAc} were chosen. A 2_{III}^{3-1} fractional factorial design was used. A detailed description of this design is provided in the supplemental methods, and an overview of the two 2_{III}^{3-1} fractional factorial designs and the resulting schemes can be found in Tables S1–S4. For the third model, where solely the effect of the addition of the trace metals Se and W was studied, a simple 2^1, also called a one-factor design, was used, with one run at the "low" level (no Se and W) and one run at the "high" level (Se and W supplied).

Since the data for each condition extended across multiple days, a permutation test was conducted separately for each experimental condition, reactor, and product (acetate, butyrate, caproate, and CH_4) in Python (v.3.10.3) to assess the significance of the time-dependent trend. A full description of the permutation test is given in the supplemental methods. The full scripts, including all parameters and preprocessing steps, are documented under resource availability.

To gain insight into what independent variables play a significant role in the production of acetate, butyrate, caproate, and CH_4 in MES, an MLRM approach was used, using "statsmodels.regression.mixed_linear_model.MixedLM" in Python (v.3.10.3). To detect multicollinearity in the regression models, the variance inflation factor (VIF) from "statsmodels.stats.outliers_influence.variance_inflation_factor" was used before regression. The MLRM was specified with the response variable as a function of the fixed effects (e.g., f'{product} ~ Factor1 + Factor2'), while reactors were included as a grouping factor for random effects (groups = "Reactor"). A random intercept model was implemented by setting "re_formula = 1," allowing each reactor to have an independent intercept without the inclusion of random slopes. The model was fitted using maximum likelihood estimation ("reml = False") with the L-BFGS optimization algorithm, and the maximum number of iterations was set to 1,000 ("maxiter = 1,000") to facilitate convergence. For each model, the marginal and conditional R^2 were determined, and predicted vs. observed values plots, residual plots, and Q-Q plots were generated to assess model quality.[18,62,63] The interpretation of the VIF, marginal and conditional R^2, and regression model validation checks is described in the supplemental methods. The full scripts, including all parameters and preprocessing steps, are documented under resource availability.

RESOURCE AVAILABILITY

Lead contact

Requests for further information, resources, and materials should be directed to and will be fulfilled by the lead contact, Ludovic Jourdin (l.jourdin@tudelft.nl).

Materials availability

This study did not generate new unique materials.

Data and code availability

- Source data (the full permutation test dataset and the DoE table used for the mixed linear regression modeling) have been deposited at 4TU.ResearchData and are publicly available as of the date of publication at https://doi.org/10.4121/5e840d08-55f6-4daa-a639-048cebcd8266.
- All original code has been deposited at 4TU.ResearchData and is publicly available at https://doi.org/10.4121/5e840d08-55f6-4daa-a639-048cebcd8266 as of the date of publication.
- Any additional information required to reanalyze the data reported in this paper is available from the lead contact upon request.

ACKNOWLEDGMENTS

The authors acknowledge Samuel P.C. Zegers and Prof. Dr. Ir. Geurt Jongbloed for invaluable expertise and guidance in developing the statistical models. This project was partly funded by the Department of Biotechnology (TU Delft) in the framework of the Zero Emission Biotechnology program and partly from the project "e-Heat: Understanding and controlling heat to enable large scale electrolysers" (NWO OTP 19757).

AUTHOR CONTRIBUTIONS

M.A.J.Z., conceptualization, methodology, software, validation, formal analysis, investigation, data curation, writing – original draft, writing – review & editing, visualization, and project administration; M.R., investigation and writing – review & editing; L.J., conceptualization, validation, resources, writing – review & editing, supervision, project administration, and funding acquisition.

DECLARATION OF INTERESTS

The authors declare no competing interests.

SUPPLEMENTAL INFORMATION

Supplemental information can be found online at https://doi.org/10.1016/j.xcrp.2025.102934.

Received: June 19, 2025
Revised: September 11, 2025
Accepted: October 10, 2025
Published: November 12, 2025

REFERENCES

1. Calvin, K., Dasgupta, D., Krinner, G., Mukherji, A., Thorne, P.W., Trisos, C., Romero, J., Aldunce, P., Barrett, K., Blanco, G., et al. (2023). IPCC, 2023: Climate Change 2023: Synthesis Report. In Contribution of Working Groups I, II and III to the Sixth Assessment Report of the Intergovernmental Panel on Climate Change [Core Writing Team, H. Lee and J. Romero, eds. (IPCC). https://doi.org/10.59327/IPCC/AR6-9789291691647.
2. Sims, R.E.H., Rogner, H.H., and Gregory, K. (2003). Carbon emission and mitigation cost comparisons between fossil fuel, nuclear and renewable energy resources for electricity generation. Energy Policy *31*, 1315–1326. https://doi.org/10.1016/S0301-4215(02)00192-1.
3. Centi, G., Iaquaniello, G., and Perathoner, S. (2019). Chemical engineering role in the use of renewable energy and alternative carbon sources in chemical production. BMC Chem. Eng. *1*, 5. https://doi.org/10.1186/s42480-019-0006-8.
4. Gao, D., Li, W., Wang, H., Wang, G., and Cai, R. (2022). Heterogeneous Catalysis for CO2 Conversion into Chemicals and Fuels. Trans. Tianjin Univ. *28*, 245–264. https://doi.org/10.1007/s12209-022-00326-x.
5. Rabaey, K., and Rozendal, R.A. (2010). Microbial electrosynthesis — revisiting the electrical route for microbial production. Nat. Rev. Microbiol. *8*, 706–716. https://doi.org/10.1038/nrmicro2422.
6. Lovley, D.R., and Nevin, K.P. (2013). Electrobiocommodities: powering microbial production of fuels and commodity chemicals from carbon dioxide with electricity. Curr. Opin. Biotechnol. *24*, 385–390. https://doi.org/10.1016/j.copbio.2013.02.012.
7. Jourdin, L., and Strik, D. (2017). Electrodes for cathodic microbial electrosynthesis processes: Key developments and criteria for effective research and implementation. In Functional Electrodes for Enzymatic and Microbial Electrochemical Systems. https://doi.org/10.1142/9781786343543_0012.
8. Jourdin, L., and Burdyny, T. (2021). Microbial Electrosynthesis: Where Do We Go from Here? Trends Biotechnol. *39*, 359–369. https://doi.org/10.1016/j.tibtech.2020.10.014.
9. Prévoteau, A., Carvajal-Arroyo, J.M., Ganigué, R., and Rabaey, K. (2020). Microbial electrosynthesis from CO2: forever a promise? Curr. Opin. Biotechnol. *62*, 48–57. https://doi.org/10.1016/j.copbio.2019.08.014.
10. Blasco-Gómez, R., Ramió-Pujol, S., Bañeras, L., Colprim, J., Balaguer, M. D., and Puig, S. (2019). Unravelling the factors that influence the bio-electrorecycling of carbon dioxide towards biofuels. Green Chem. *21*, 684–691. https://doi.org/10.1039/C8GC03417F.
11. Vassilev, I., Dessì, P., Puig, S., and Kokko, M. (2022). Cathodic biofilms – A prerequisite for microbial electrosynthesis. Bioresour. Technol. *348*, 126788. https://doi.org/10.1016/j.biortech.2022.126788.
12. Das, S., Das, I., and Ghangrekar, M.M. (2020). Role of applied potential on microbial electrosynthesis of organic compounds through carbon dioxide sequestration. J. Environ. Chem. Eng. *8*, 104028. https://doi.org/10.1016/j.jece.2020.104028.
13. Rovira-Alsina, L., Balaguer, M.D., and Puig, S. (2021). Thermophilic bio-electro carbon dioxide recycling harnessing renewable energy surplus. Bioresour. Technol. *321*, 124423. https://doi.org/10.1016/j.biortech.2020.124423.
14. Korth, B., and Harnisch, F. (2019). In Modeling Microbial Electrosynthesis, D. Holtmann, ed. (Springer International Publishing), pp. 273–325. https://doi.org/10.1007/10_2017_35.
15. Gadkari, S., Shemfe, M., Modestra, J.A., Mohan, S.V., and Sadhukhan, J. (2019). Understanding the interdependence of operating parameters in microbial electrosynthesis: a numerical investigation. Phys. Chem. Chem. Phys. *21*, 10761–10772. https://doi.org/10.1039/C9CP01288E.
16. Li, C., Li, H., Li, P., Dang, Y., Sun, D., and Guo, D. (2024). Enhancing Predictions of Acetate and Ethanol Production from Microbial Electrosynthesis Using Optimized Machine Learning Models. ACS Sustain. Chem. Eng. *12*, 4264–4275. https://doi.org/10.1021/acssuschemeng.3c08356.
17. Cabau-Peinado, O., Straathof, A.J.J., and Jourdin, L. (2021). A General Model for Biofilm-Driven Microbial Electrosynthesis of Carboxylates From CO2. Front. Microbiol. *12*, 669218. https://doi.org/10.3389/fmicb.2021.669218.
18. Montgomery, D.C. (2017). Montgomery: Design and Analysis of Experiments.
19. Kracke, F., Deutzmann, J.S., Jayathilake, B.S., Pang, S.H., Chandrasekaran, S., Baker, S.E., and Spormann, A.M. (2021). Efficient Hydrogen Delivery for Microbial Electrosynthesis via 3D-Printed Cathodes. Front. Microbiol. *12*, 696473. https://doi.org/10.3389/fmicb.2021.696473.
20. Jourdin, L., Winkelhorst, M., Rawls, B., Buisman, C.J.N., and Strik, D.P.B. T.B. (2019). Enhanced selectivity to butyrate and caproate above acetate in continuous bioelectrochemical chain elongation from CO2: Steering with CO2 loading rate and hydraulic retention time. Bioresour. Technol. Rep. *7*, 100284. https://doi.org/10.1016/j.biteb.2019.100284.
21. Lund, P.A., De Biase, D., Liran, O., Scheler, O., Mira, N.P., Cetecioglu, Z., Fernández, E.N., Bover-Cid, S., Hall, R., Sauer, M., and O'Byrne, C. (2020). Understanding How Microorganisms Respond to Acid pH Is Central to Their Control and Successful Exploitation. Front. Microbiol. *11*, 556140. https://doi.org/10.3389/fmicb.2020.556140.
22. Sun, M., Gao, A.X., Liu, X., Bai, Z., Wang, P., and Ledesma-Amaro, R. (2024). Microbial conversion of ethanol to high-value products: progress and challenges. Biotechnol. Biofuels Bioprod. *17*, 115. https://doi.org/10.1186/s13068-024-02546-w.
23. Muñoz-Duarte, L., Chakraborty, S., Grøn, L.V., Bambace, M.F., Catalano, J., and Philips, J. (2024). H2 Consumption by Various Acetogenic Bacteria Follows First-Order Kinetics up to H2 Saturation. Biotechnol. Bioeng. *122*, 804–816. https://doi.org/10.1002/BIT.28904.
24. Zhu, X., and Tan, X. (2009). Metalloproteins/metalloenzymes for the synthesis of acetyl-CoA in the Wood-Ljungdahl pathway. Sci. China B Chem. *52*, 2071–2082. https://doi.org/10.1007/s11426-009-0082-3.
25. Ammam, F., Tremblay, P.-L., Lizak, D.M., and Zhang, T. (2016). Effect of tungstate on acetate and ethanol production by the electrosynthetic bacterium Sporomusa ovata. Biotechnol. Biofuels *9*, 163. https://doi.org/10.1186/s13068-016-0576-0.
26. Saxena, J., and Tanner, R.S. (2011). Effect of trace metals on ethanol production from synthesis gas by the ethanologenic acetogen, Clostridium ragsdalei. J. Ind. Microbiol. Biotechnol. *38*, 513–521. https://doi.org/10.1007/s10295-010-0794-6.
27. Twisk, J.W.R. (2019). Applied Mixed Model Analysis. https://doi.org/10.1017/9781108635660.
28. Zegers, M.A.J., Augustijn, E., Jongbloed, G., and Jourdin, L. (2025). Novel miniaturised microbial electrosynthesis reactor: A study on replicability. Chem. Eng. J. *516*, 163881. https://doi.org/10.1016/j.cej.2025.163881.
29. Cabau-Peinado, O., Winkelhorst, M., Stroek, R., de Kat Angelino, R., Straathof, A.J.J., Masania, K., Daran, J.M., and Jourdin, L. (2024). Microbial electrosynthesis from CO2 reaches productivity of syngas and chain elongation fermentations. Trends Biotechnol. *42*, 1503–1522. https://doi.org/10.1016/J.TIBTECH.2024.06.005.
30. Raes, S.M.T., Jourdin, L., Buisman, C.J.N., and Strik, D.P.B.T.B. (2017). Continuous Long-Term Bioelectrochemical Chain Elongation to Butyrate. Chemelectrochem *4*, 386–395. https://doi.org/10.1002/celc.201600587.
31. Jourdin, L., Freguia, S., Flexer, V., and Keller, J. (2016). Bringing High-Rate, CO $_2$ -Based Microbial Electrosynthesis Closer to Practical Implementation through Improved Electrode Design and Operating Conditions. Environ. Sci. Technol. *50*, 1982–1989. https://doi.org/10.1021/acs.est.5b04431.
32. LaBelle, E.V., and May, H.D. (2017). Energy efficiency and productivity enhancement of microbial electrosynthesis of acetate. Front. Microbiol. *8*, 756. https://doi.org/10.3389/fmicb.2017.00756.
33. Marshall, C.W., Ross, D.E., Handley, K.M., Weisenhorn, P.B., Edirisinghe, J.N., Henry, C.S., Gilbert, J.A., May, H.D., and Norman, R.S. (2017).

Metabolic reconstruction and modeling microbial electrosynthesis. Sci. Rep. *7*, 8391. https://doi.org/10.1038/s41598-017-08877-z.

34. Ganigué, R., Sánchez-Paredes, P., Bañeras, L., and Colprim, J. (2016). Low Fermentation pH Is a Trigger to Alcohol Production, but a Killer to Chain Elongation. Front. Microbiol. *7*, 702. https://doi.org/10.3389/fmicb.2016.00702.
35. Rojas, M., del, P.A., Zaiat, M., González, E.R., De Wever, H., and Pant, D. (2021). Enhancing the gas–liquid mass transfer during microbial electrosynthesis by the variation of CO2 flow rate. Process Biochem. *101*, 50–58. https://doi.org/10.1016/j.procbio.2020.11.005.
36. Ganigué, R., Puig, S., Batlle-Vilanova, P., Balaguer, M.D., and Colprim, J. (2015). Microbial electrosynthesis of butyrate from carbon dioxide. Chem. Commun. *51*, 3235–3238. https://doi.org/10.1039/C4CC10121A.
37. Daniell, J., Köpke, M., and Simpson, S.D. (2012). Commercial biomass syngas fermentation. Energies *5*, 5372–5417. https://doi.org/10.3390/en5125372.
38. Raes, S.M.T., Jourdin, L., Buisman, C.J.N., and Strik, D.P.B.T.B. (2020). Bioelectrochemical Chain Elongation of Short-Chain Fatty Acids Creates Steering Opportunities for Selective Formation of n-Butyrate, n-Valerate or n-Caproate. ChemistrySelect *5*, 9127–9133. https://doi.org/10.1002/slct.202002001.
39. González-Cabaleiro, R., Lema, J.M., Rodríguez, J., and Kleerebezem, R. (2013). Linking thermodynamics and kinetics to assess pathway reversibility in anaerobic bioprocesses. Energy Environ. Sci. *6*, 3780. https://doi.org/10.1039/c3ee42754d.
40. Winkelhorst, M., Cabau-Peinado, O., Straathof, A.J.J., and Jourdin, L. (2023). Biomass-specific rates as key performance indicators: A nitrogen balancing method for biofilm-based electrochemical conversion. Front. Bioeng. Biotechnol. *11*, 1096086. https://doi.org/10.3389/fbioe.2023.1096086.
41. Parera Olm, I., and Sousa, D.Z. (2023). Upgrading dilute ethanol to odd-chain carboxylic acids by a synthetic co-culture of Anaerotignum neopropionicum and Clostridium kluyveri. Biotechnol. Biofuels Bioprod. *16*, 83. https://doi.org/10.1186/s13068-023-02336-w.
42. Vasudevan, D., Richter, H., and Angenent, L.T. (2014). Upgrading dilute ethanol from syngas fermentation to n-caproate with reactor microbiomes. Bioresour. Technol. *151*, 378–382. https://doi.org/10.1016/j.biortech.2013.09.105.
43. Rago, L., Ruiz, Y., Baeza, J.A., Guisasola, A., and Cortés, P. (2015). Microbial community analysis in a long-term membrane-less microbial electrolysis cell with hydrogen and methane production. Bioelectrochemistry *106*, 359–368. https://doi.org/10.1016/j.bioelechem.2015.06.003.
44. Bian, B., Xu, J., Katuri, K.P., and Saikaly, P.E. (2021). Resistance assessment of microbial electrosynthesis for biochemical production to changes in delivery methods and CO2 flow rates. Bioresour. Technol. *319*, 124177. https://doi.org/10.1016/j.biortech.2020.124177.
45. Mills, S., Dessì, P., Pant, D., Farràs, P., Sloan, W.T., Collins, G., and Ijaz, U. Z. (2022). A meta-analysis of acetogenic and methanogenic microbiomes in microbial electrosynthesis. NPJ Biofilms Microbio. *8*, 73. https://doi.org/10.1038/s41522-022-00337-5.
46. Scholten, J.C.M., Conrad, R., and Stams, A.J.M. (2000). Effect of 2-bromo-ethane sulfonate, molybdate and chloroform on acetate consumption by methanogenic and sulfate-reducing populations in freshwater sediment. FEMS Microbiol. Ecol. *32*, 35–42. https://doi.org/10.1016/S0168-6496(00)00006-4.
47. Zhou, H., Xing, D., Xu, M., Su, Y., Ma, J., Angelidaki, I., and Zhang, Y. (2021). Optimization of a newly developed electromethanogenesis for the highest record of methane production. J. Hazard. Mater. *407*, 124363. https://doi.org/10.1016/J.JHAZMAT.2020.124363.
48. Kovalev, A.A., Kovalev, D.A., Zhuravleva, E.A., Katraeva, I.V., Panchenko, V., Fiore, U., and Litti, Y.V. (2022). Two-stage anaerobic digestion with direct electric stimulation of methanogenesis: The effect of a physical barrier to retain biomass on the surface of a carbon cloth-based biocathode. Renew. Energy *181*, 966–977. https://doi.org/10.1016/J.RENENE.2021.09.097.
49. Pelaz, G., Carrillo-Peña, D., Morán, A., and Escapa, A. (2024). Microbial electromethanogenesis for energy storage: Influence of acidic pH on process performance. J. Energy Storage *75*, 109685. https://doi.org/10.1016/J.EST.2023.109685.
50. Karekar, S., Stefanini, R., and Ahring, B. (2022). Homo-Acetogens: Their Metabolism and Competitive Relationship with Hydrogenotrophic Methanogens. Microorganisms *10*, 397. https://doi.org/10.3390/microorganisms10020397.
51. Dessì, P., Sánchez, C., Mills, S., Cocco, F.G., Isipato, M., Ijaz, U.Z., Collins, G., and Lens, P.N.L. (2021). Carboxylic acids production and electrosynthetic microbial community evolution under different CO2 feeding regimens. Bioelectrochemistry *137*, 107686. https://doi.org/10.1016/J.BIOELECHEM.2020.107686.
52. Batlle-Vilanova, P., Ganigué, R., Ramió-Pujol, S., Bañeras, L., Jiménez, G., Hidalgo, M., Balaguer, M.D., Colprim, J., and Puig, S. (2017). Microbial electrosynthesis of butyrate from carbon dioxide: Production and extraction. Bioelectrochemistry *117*, 57–64. https://doi.org/10.1016/j.bioelechem.2017.06.004.
53. He, Y., Cassarini, C., and Lens, P.N.L. (2021). Bioethanol Production From H2/CO2 by Solventogenesis Using Anaerobic Granular Sludge: Effect of Process Parameters. Front. Microbiol. *12*, 647370. https://doi.org/10.3389/fmicb.2021.647370.
54. Molenaar, S.D., Saha, P., Mol, A.R., Sleutels, T.H.J.A., ter Heijne, A., and Buisman, C.J.N. (2017). Competition between methanogens and acetogens in biocathodes: A comparison between potentiostatic and galvanostatic control. Int. J. Mol. Sci. *18*, 204. https://doi.org/10.3390/ijms18010204.
55. Joshi, A., Lanjekar, V., Dhakephalkar, P.K., and Dagar, S.S. (2018). Cultivation of multiple genera of hydrogenotrophic methanogens from different environmental niches. Anaerobe *50*, 64–68. https://doi.org/10.1016/J.ANAEROBE.2018.02.001.
56. Siegert, M., Yates, M.D., Spormann, A.M., and Logan, B.E. (2015). Methanobacterium Dominates Biocathodic Archaeal Communities in Methanogenic Microbial Electrolysis Cells. ACS Sustain. Chem. Eng. *3*, 1668–1676. https://doi.org/10.1021/ACSSUSCHEMENG.5B00367/SUPPL_FILE/SC5B00367_SI_001.PDF.
57. An, T., and Kim, Y.K. (2022). Effect of selenium and tungsten on cell growth and metabolite production in syngas fermentation using "Clostridium autoethanogenum.". J. Biotechnol. *356*, 60–64. https://doi.org/10.1016/j.jbiotec.2022.07.004.
58. Shin, J., Song, Y., Jeong, Y., and Cho, B.K. (2016). Analysis of the core genome and pan-genome of autotrophic acetogenic bacteria. Front. Microbiol. *7*, 188448. https://doi.org/10.3389/FMICB.2016.01531/BIBTEX.
59. Yamamoto, I., Saiki, T., Liu, S.M., and Ljungdahl, L.G. (1983). Purification and properties of NADP-dependent formate dehydrogenase from Clostridium thermoaceticum, a tungsten-selenium-iron protein. J. Biol. Chem. *258*, 1826–1832. https://doi.org/10.1016/S0021-9258(18)33062-X.
60. Chaitanya, N.K., Thulluru, L.P., and Chatterjee, P. (2023). Optimization of Long-Chain Fatty Acid Synthesis from CO 2 Using Response Surface Methodology. J. Hazard. Toxic Radioact. Waste *27*, 04023017. https://doi.org/10.1061/JHTRBP.HZENG-1229/SUPPL_FILE/SUPPLEMENTAL_MATERIALS_JHTRBP.HZENG-1229_CHAITANYA.PDF.
61. Chakraborty, S., Rene, E.R., Lens, P.N.L., Rintala, J., Veiga, M.C., and Kennes, C. (2020). Effect of tungsten and selenium on C1 gas bioconversion by an enriched anaerobic sludge and microbial community analysis. Chemosphere *250*, 126105. https://doi.org/10.1016/J.CHEMOSPHERE.2020.126105.
62. Montgomery, D.C., Peck, E.A., and Vining, G.G. (2012). Introduction to Linear Regression Analysis, Fifth Edition (John Wiley & Sons).
63. Nakagawa, S., and Schielzeth, H. (2013). A general and simple method for obtaining R2 from generalized linear mixed-effects models. Methods Ecol. Evol. *4*, 133–142. https://doi.org/10.1111/j.2041-210x.2012.00261.x.